Regular Article – Plasma Physics

On different modes of a filamentary atmospheric pressure plasma jet: modeling, laser schlieren deflectometric and high-speed camera investigations

Thorben Wolff[1,2,a] , Rüdiger Foest[2], and Holger Kersten[1]

[1] Institute of Experimental and Applied Physics, Kiel University, Leibnizstraße 11-19, 24098 Kiel, Germany
[2] Leibniz Institute for Plasma Science and Technology (INP), Felix-Hausdorff-Str. 2, 17489 Greifswald, Germany

Abstract. We investigated a filamentary non-thermal atmospheric pressure plasma jet used for coating applications. The plasma jet exhibits two different modes, the stationary mode and the locked mode, in which the filaments rotate around the plasma jet axis. We present a model for the modes and verify it by measurements with high-speed camera and laser schlieren deflectometry. Laser schlieren deflectometry investigations reveal a drift of the rotation frequency over time towards lower values. Additionally, relations between the filament rotation frequency and gas flow as well as input power, respectively, are investigated by the laser schlieren deflectometry. Correlation between rotation frequency and gas flow show a linear dependence and with increasing power the rotation frequency increases as well. All the results are in agreement with the proposed model.

1 Introduction

Thin film coatings are utilized in a wide range of applications in order to provide surface properties that the solid raw material cannot provide. These properties include among others wear resistance, easy-to-clean surfaces and barrier properties against heat or diffusion. Plasmas, and particularly atmospheric pressure plasma jets, have proven to be a very suitable tool for providing tailored coatings [1–4].

An example for a typical atmospheric pressure plasma jet, which has been proven suitable for homogeneous coatings, is the filamentary non-thermal atmospheric pressure plasma jet described by Schäfer et al. [5]. This cylindrical filamentary plasma jet exhibits different modes depending on the discharge parameters. Of particular interest are the stationary mode and the locked mode. In the stationary mode the filaments are static and do not move. Additionally, if more than one filament is present, the filaments are distributed symmetrically around the jet axis. In the locked mode, on the other hand, the filaments move around the jet axis, while still maintaining a symmetric distribution. This plasma jet was investigated in different studies and the advantages of the locked mode for the homogeneity of coatings were clearly shown [6–8]. The basics of both modes were investigated in detail in [9]. Recently, the

locked mode was investigated in a paper of Schäfer et al. [10] where they present the same relation between the inclination of the rotating filaments and the speed of the gas flow through the plasma jet as shown in [9].

Besides a modification of the model for describing the behavior of the filaments, we present here experimentally obtained results for the validation of the model predictions regarding filament motion, for the influence of power and gas flow as well as for the transition between both modes. The dynamics of the plasma jet were examined with high-speed cameras. Furthermore, laser schlieren deflectometry was applied to measure the rotation frequency of the filaments in the locked mode for different discharge parameters. Laser schlieren deflectometry uses variations of the refractive index in the effluent of the plasma jet due to temperature variations induced by the filaments (see [11]).

2 Experimental setup

2.1 Atmospheric pressure plasma jet

The plasma jet used and investigated in this work is shown in Fig. 1. It consists of a cylindrical glass body, inner diameter 4 mm, surrounded by two copper electrodes with a distance of 4.8 mm and an inner ceramic capillary, outer diameter 1.8 mm, for additional precursor gases, e.g., for coating purposes. The upstream electrode is rf-powered (27.12 MHz) and connected to the power supply via a matching network. The downstream

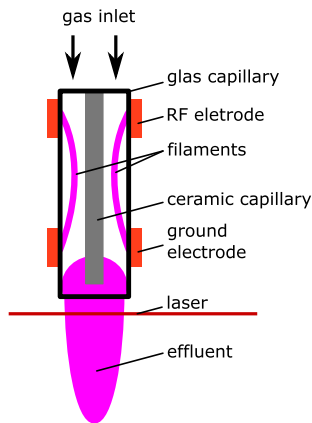[a] e-mail: thorben.wolff.physik@gmail.com (corresponding author)

Fig. 1 Schematic of the atmospheric pressure plasma jet. The laser for the laser schlieren deflectometry is shown passing through the effluent

electrode is grounded. Both electrodes are water-cooled. The working gas is argon. Ten of these jets are operated simultaneously next to each other with one power supply for large area treatment.

The results presented in this work are all obtained from just one plasma jet. The plasma jets have filamentary discharges with different modes. The filaments are either stationary (stationary mode) or rotate around the plasma jet axis (locked mode). If there is more than one filament, they are distributed symmetrically around the jet axis, independent on the mode. In this work, only the modes with three filaments were considered.

2.2 Laser schlieren deflectometry

The rotation frequency of the plasma jet is investigated by the laser schlieren deflectometry described in [11]. The discharges in form of the filaments raise the temperature in the discharge volume. The temperature variations and gradients between the species from the discharge volume and their surroundings persists in the effluent. This effect leads to differences in the refractive index. A laser pointed through the effluent (Fig. 1) will be deflected due to these differences. With the plasma jet in locked mode, this deflection is periodically changing. A photodiode placed in the center of the undisturbed laser measures the deflection due to intensity variations. The shown frequencies of the deflection correspond to the rotation frequencies of the filaments multiplied by the number of filaments.

2.3 High-speed camera

High-speed video analysis of the filament dynamics was carried out with a camera IDT Motion Pro Y4 from Imaging Solutions GmbH set to 1500 fps with an exposure time of 14 μs. The transition between modes was examined with a Panasonic lumix dmc-fz100 set to 200 fps.
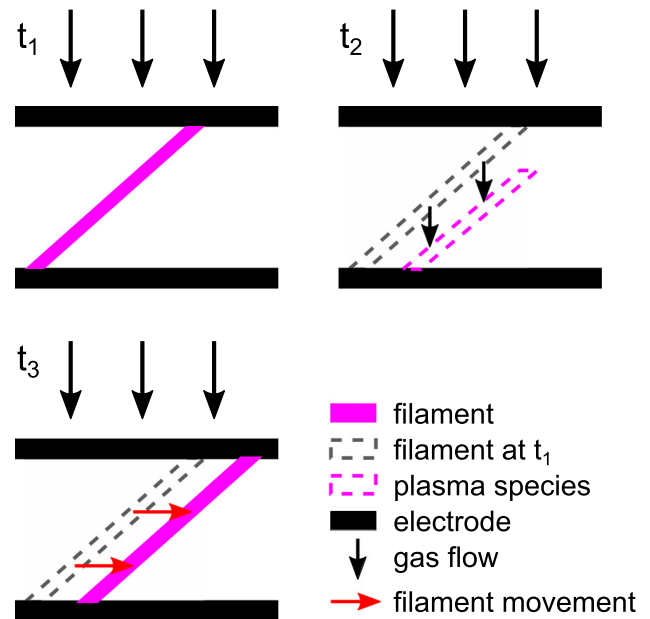

Fig. 2 Illustration of the filament propagation between the electrodes. At time t_1 the filament is located between the electrodes. The gas flow moves the plasma species downstream (time t_2) and the filament moves accordingly (t_3) but stays between the electrodes resulting in a sideways motion of the filament

3 Suggestion of a simple model for the modes of the plasma jet

Firstly, we are assuming that the length of the filaments correlates to the input power. Correlations between the input power and the plasma volume have already been reported earlier [6, 12, 13]. Secondly, we are supposing that the attachment zone of the filament at the upstream electrode dominates the behavior of the filament. The latter assumption is supported by the fluid dynamics of plasma jets in general. The transport of plasma species and, therefore, the geometry of the plasma jet are dependent on the gas flow. Accordingly, the gas flow transports the species of the plasma filament downstream and, thereby, the energetically favorable position for the filament is defined. We now consider an inclined filament with a constant length L as shown in Fig. 2 at time t_1. The plasma species move downstream together with the gas flow following the conservation of momentum (time t_2). The new location of these species is the energetically favorable spot for the filament. Keeping a constant length will result in the upstream attachment point and by that the whole filament is moving sideways (time t_3).

The velocity of the filament v_F can be calculated using the velocity of the gas v_{gas}, the distance d of the electrodes and the length of the filament L (see Fig. 3):
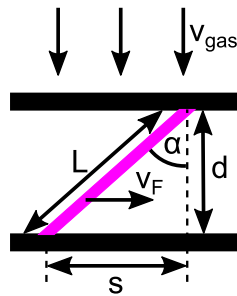
$$v_F = v_{gas}\sqrt{\frac{L^2}{d^2} - 1}$$

Fig. 3 Illustration for the relation between the filament movement v_F, the length of the filament L and its inclination α, the distance of the electrodes d and the velocity of the gas v_gas

Consequently, the rotation frequency f is:

$$f = \frac{v_\mathrm{gas}}{2\pi R}\sqrt{\frac{L^2}{d^2} - 1}$$

R denotes the radius of the filament circulation, i.e., inner radius of the glass capillary in maximum.

This explanation has different consequences for the description of the plasma jet and its modes. Assuming an increasing filament length with increasing input power, starting at zero, the plasma will ignite at a certain power, sufficient for one filament with the length equal to the distance of the electrodes. This filament has no inclination and, therefore, does not move. The jet is in the stationary mode. Increasing the power further will lead to a longer filament with an inclination different from zero which will move according to the situation described above. The jet is in the locked mode. The transition from the stationary to the locked mode is described in more detail in the next section. Increasing the power even further will result in a longer filament with higher inclination and a faster rotation of the filament. At some point, the power is sufficiently high for filament length of twice the electrode distance. A second filament will form and the jet is in the stationary mode with two filaments. The process repeats itself with an increasing number of filaments for further increases of the input power.

The fundamental model was first proposed in [9]. Recently, Schäfer et al. presented the same relation connecting the rotation frequency to the gas flow and inclination of the filaments, though they start at the conservation of the temperature inside the filament [10]. However, their model starts with inclined filaments and, hence, does only explain the locked mode, whereas the model presented in this work may also explain the stationary mode and the transition between the modes. Experimentally, the succession of modes was described by Schäfer et al. [5].

4 Results and discussion

Now, the proposed model is based on the coupling of the dynamics of the plasma filaments to the gas flow.
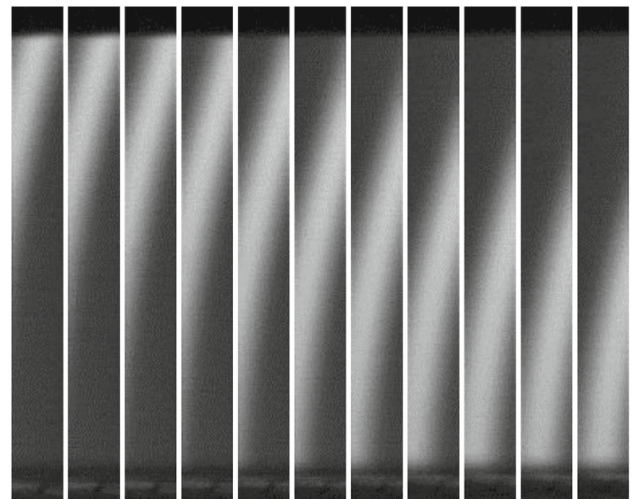
(a)
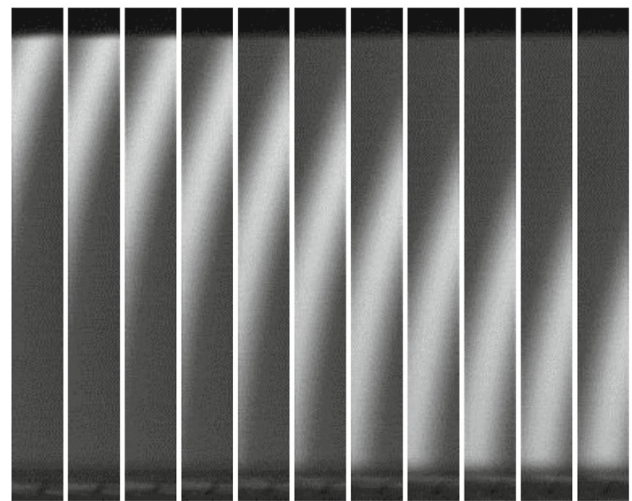
(b)

Fig. 4 High-speed camera images of rotating filaments at **a** 5.6 W and **b** 6.6 W. The camera was set to 1500 fps with an exposure time of 14 μs. Despite the different rotating frequencies of **a** 45 Hz and **b** 68 Hz a time difference for the filaments crossing the section shown is not discernable

Hence, the motion of the plasma parallel to the jet axis should only depend on the gas flow and should be independent on the applied power. On the same time, an increase in the applied power should increase the frequency. For verification of the model high-speed camera investigations of the plasma jet were carried out with the camera IDT Motion Pro Y4 from Imaging Solutions GmbH. The plasma jet was operated in the locked mode with three filaments with a gas flow of 0.13 slm in the outer capillary. A sample frequency of 1500 fps was used. Figure 4 shows the filament progress for two different powers, 5.6 W and 6.6 W, with corresponding rotation frequencies of 45 Hz and 68 Hz, respectively. Despite the increase in the rotation frequency of around 50% the time Δt between the top and the bottom part

Table 1 Results of filament propagation investigations with the high-speed camera IDT Motion Pro Y4 from Imaging Solutions GmbH. The plasma jet was operated in the locked mode with three filaments with a gas flow of 0.13 slm in the outer and 0 slm in the inner capillary. The camera was set to 1500 fps with an exposure time of 14 μs

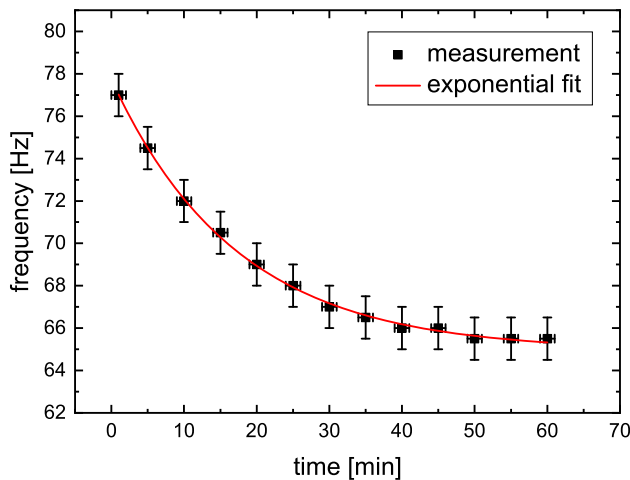| Power (W)	Time Δt (s)	Standard deviation of Δt (s)	Frequency (Hz)	Standard deviation of the frequency (Hz)
5.6	$6.8 \cdot 10^{-3}$	$0.2 \cdot 10^{-3}$	45	1
6.6	$6.5 \cdot 10^{-3}$	$0.2 \cdot 10^{-3}$	68	1
7.6	$6.2 \cdot 10^{-3}$	$0.2 \cdot 10^{-3}$	75	1

Fig. 5 Course of the frequency over time after starting the plasma jet and setting it to locked mode for three filaments. The frequency decreases exponentially for about 50 min. The measurements were done with an outer gas flow of 0.19 slm Ar, a power of 8 W and a gas flow of 0.05 slm Ar through the inner capillary

Fig. 6 Dependence of the filament frequency (three filaments) on the gas flow through the outer capillary. The trend is linear. The results were obtained with a power of 7.7 W and without a gas flow through the inner capillary after a warm up time of 100 min

of the filament reaching the same point along the jet axis is the same.

Additional analysis of the light intensities leads to the results shown in Table 1. The time difference is almost the same for all three frequencies. This shows that the plasma motion is dominated by the gas flow and independent on the applied power. Changes in the rotation frequency due to power changes are a consequence of the increased filament length and subsequent formation of additional filaments.

The effects of the gas flow and the discharge power were investigated by laser schlieren deflectometry. During these experiments a drift of the frequency to lower numbers over time was noticed (see Fig. 5). The rotation frequency of the filaments slows down exponentially for constant power and gas flow. After about 1 h, the frequency is almost stable. Our hypothesis for this drift focusses on the matching network between the rf power supply and the plasma jet. The matching network heats up during the experiments. This changes the resonance frequency and the ratio of the power feed into the plasma also changes. With decreasing power the rotation frequency decreases as well.
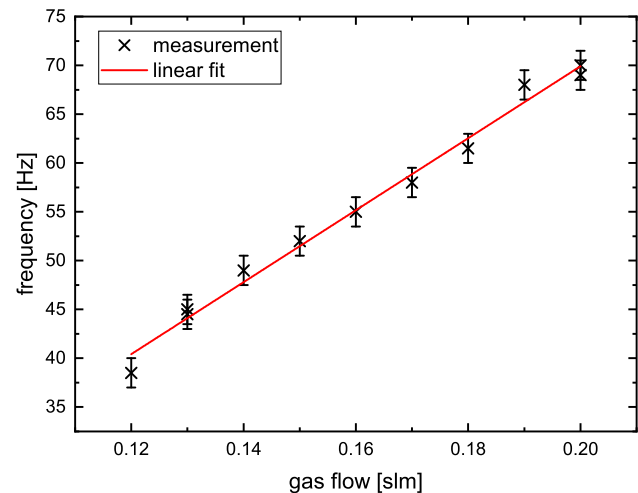
The influence of the gas flow was investigated for a power of 7.7 W for the single jet. Because of the drift of the frequency discussed above, the jet heated up for about 100 min before the actual experiments. The results are shown in Fig. 6. The linear trend clearly confirms the expectation from the model.

Repetitive measurements show no drift signifying that the gas flow is not influencing the drift notably. The great influence of the gas flow makes it an excellent parameter to adjust the rotation frequency to a desired value.

The influence of the gas flow was also investigated by Schäfer et al. [5]. Though the frequency also increased with increasing gas flow, the relation did not seem to be linear. However, just a few points were presented for different powers and there was no mention of a drift or the plasma source heating up before the measurements. Therefore, the drift could explain the slightly different results.

The second parameter influencing the rotation frequency is the applied power. A gas flow of 0.13 slm was used. The plasma jet was operated at 7.7 W for 130 min before the frequency was stable. Since different powers could influence the drift, the measurements were carried out with increasing powers and directly
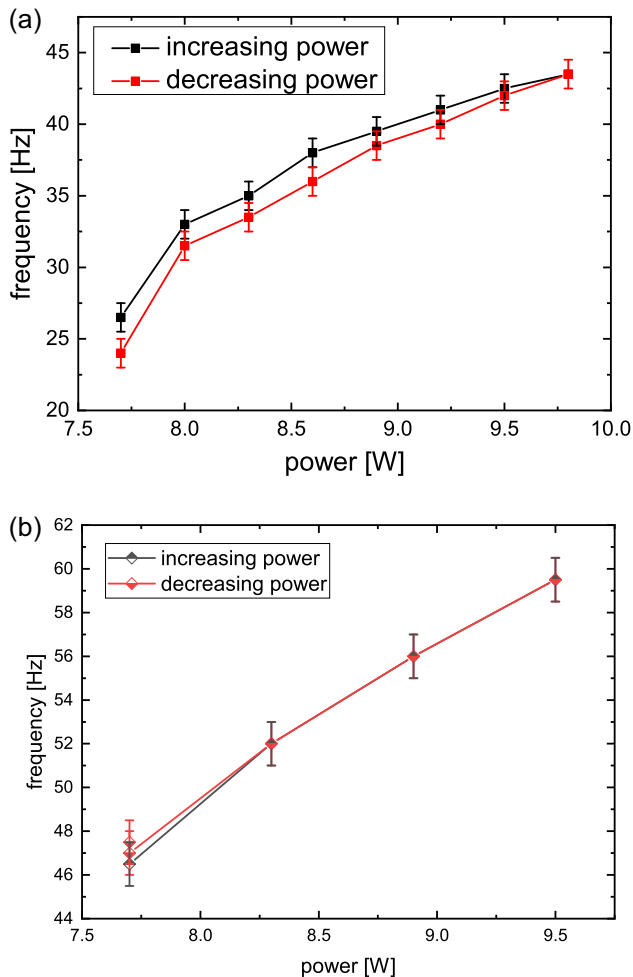
Fig. 7 Dependence of the filament frequency (three filaments) on the applied power. The results exhibit a strong influence of the power. The results in (**a**) show a small hysteresis (0.13 slm outer gas flow, 0 slm inner gas flow, 130 min warm-up at 7.7 W). The results in (**b**) show no hysteresis at higher gas flow (0.16 slm outer gas flow, 0 slm inner gas flow, 65 min warm-up at 7.7 W). For both measurements the power was increased and after reaching the highest point decreased again

afterward repeated with decreasing powers. The results are presented in Fig. 7a. They show that the frequency increases with the power as already observed with the high-speed camera measurements. This, together with the high-speed camera measurements, supports the assumption that increasing powers lead to longer filaments and, therefore, higher filament inclinations. This is also supported by the findings of Schäfer et al. [10].

The difference between the results in Fig. 7a from increasing and decreasing power grows during the experiments (towards smaller powers). This hysteresis indicates that there might be a stronger drift for higher powers, resulting in lower rotation frequencies going from higher to lower powers. However, further investigation with different parameters show this effect only

sometimes, in particular, at low gas flow. The measurement series in Fig. 7b at higher gas flow shows no difference between the results for increasing and decreasing power. In conclusion, more investigations are necessary to explore the drift and possible influence of the plasma parameters. Furthermore, the power actually fed into the plasma is unknown, since there are different losses between the power supply and the plasma, e.g., the matching network. For a quantitative analysis of the correlation between input power and plasma frequency and filament length the determination of these losses is absolutely necessary.

Additional verification of the model can be achieved by a closer look at the transition from stationary mode to locked mode. High-speed camera image series of the transition are presented in Fig. 8. The plasma jet starts in stationary mode (first row). The length of the filaments L equals the distance d between the electrodes. Following the model, the filaments do not move, since the inclination to the jet axis is zero. With increasing power the plasma jet changes to the transition regime. First, the upstream attachment point of one of the filaments moves to the side causing a kink in the filament. This kink propagates through the filament until it moved completely to the side (second row). Afterward, the process repeats itself to the other side, restoring the symmetry. This demonstrates the increasing length of a filament with increasing power and the dependence of the filament on the upstream attachment point or rather the dependence of the downstream parts on those further upstream.

Further increase in power results in all filaments moving a step sideways or rotating shortly, turning around and coming back (third row). Finally, reaching the locked mode, the filaments rotate constantly along the electrodes (fourth row). The transition from locked mode to stationary mode by lowering the power follows the same steps in reversed order. This transition behavior is in good agreement with the proposed model.

5 Conclusion

A modified model for the different modes of the investigated filamentary atmospheric pressure plasma jet was proposed. The model describes both the stationary and the locked mode, in which the filaments rotate around the jet axis. Furthermore, the model can explain the transition between the modes. Experimental investigations with a high-speed camera and laser schlieren deflectometry were carried out to verify the model and its predictions. The results show clearly that the filament dynamics are dominated by the gas flow and increasing gas flow as well as power lead to rising rotation frequencies as predicted. The proposed model enhances the understanding of the physical nature of the locked mode and enables to better control the process. Future investigations need to focus on the power actually fed into the plasma and the correlation between this value and the plasma volume. Furthermore, the

Fig. 8 Image sequences of the transition between stationary and locked mode with three filaments. The gas flows through the capillary from top to bottom. The first row shows the stationary mode. The filaments do not move. In the second row, the right filament moves alternating to left and right. The movement starts at and is dominated by the point at the top electrode. The third row shows alternating movements of all filaments first to the right and then to the left. The last row finally shows the locked mode. All filaments move in one direction around the capillary. The images in one row have a time gap of 5 ms. The time between the rows is larger

origin of the drift and potential influences need to be examined further.

Authors' contribution

All authors contributed to the study conception and design. Material preparation, data collection and analysis were performed by TW. The first draft of the manuscript was written by TW and all authors commented on previous versions of the manuscript. All authors read and approved the final manuscript.

Data Availability Statement This manuscript has no associated data or the data will not be deposited. [Authors' comment: The datasets generated during and/or analyzed during the current study are available from the corresponding author on reasonable request.]

Declarations

Conflict of interest The authors declare that they have no competing interest.

References

1. M. Noborisaka, T. Mori, R. Horikoshi, A. Shirakura, A. Hashimoto, T. Suzuki, Abrasion resistance of silica-based coatings prepared by atmospheric pressure plasma chemical vapor deposition for protection of polymeric surfaces. J. Vac. Sci. Technol., A: Vac. Surf. Films **31**(6), 061508 (2013)

2. U. Lommatzsch, J. Ihde, Plasma polymerization of HMDSO with an atmospheric pressure plasma jet for corrosion protection of aluminum and low-adhesion surfaces. Plasma Processes Polym. **6**(10), 642–648 (2009)

3. C. Tendero, C. Tixier, P. Tristant, J. Desmaison, P. Leprince, Atmospheric pressure plasmas: a review. Spectrochim. Acta Part B **61**(1), 2–30 (2006)

4. H. Zhang, Z. Guo, Q. Chen, X. Wang, Z. Wang, Z. Liu, Deposition of silicon oxide coatings by atmospheric pressure plasma jet for oxygen diffusion barrier applications. Thin Solid Films **615**, 63–68 (2016)

5. J. Schäfer, R. Foest, A. Ohl, K. Weltmann, Miniaturized non-thermal atmospheric pressure plasma jet—characterization of self-organized regimes. Plasma Phys. Controll. Fus. **51**(12), 124045 (2009)

6. J. Schäfer, F. Sigeneger, R. Foest, D. Loffhagen, K.-D. Weltmann, On a non-thermal atmospheric pressure plasma jet used for the deposition of silicon-organic films. Eur. Phys. J. D **72**(5), 90 (2018)

7. J. Schäfer, F. Sigeneger, R. Foest, D. Loffhagen, K.-D. Weltmann, On plasma parameters of a self-organized plasma jet at atmospheric pressure. Eur. Phys. J. D **60**(3), 531–538 (2010)

8. A. Vogelsang, A. Ohl, R. Foest, K.D. Weltmann, Fluorocarbon plasma polymer deposition by an atmospheric pressure microplasma jet using different precursor molecules–a comparative study. Plasma Process. Polym. **10**(4), 364–371 (2013)

9. T. Kewitz, Experimentelle Untersuchungen und Simulationen an Atmosphärendruck-Plasmen. Master Thesis, Mathematisch-Naturwissenschaftliche Fakultät, Institut für Experimentelle und Angewandte Physik, Christian-Albrechts-Universität zu Kiel, 2012.

10. J. Schäfer, F. Sigeneger, J. Šperka, C. Rodenburg, R. Foest, Searching for order in atmospheric pressure plasma jets. Plasma Phys. Controll. Fusion **60**(1), 014038 (2017)

11. J. Schäfer, R. Foest, S. Reuter, T. Kewitz, J. Šperka, K.-D. Weltmann, Laser schlieren deflectometry for temperature analysis of filamentary non-thermal atmospheric pressure plasma. Rev. Sci. Instrum. **83**(10), 103506 (2012)

12. E. Stoffels, A. Flikweert, W. Stoffels, G. Kroesen, Plasma needle: a non-destructive atmospheric plasma source for fine surface treatment of (bio) materials. Plasma Sources Sci. Technol. **11**(4), 383 (2002)

13. V. Prysiazhnyi, A. Brablec, J. Čech, M. Stupavská, M. Černák, Generation of large-area highly-nonequlibrium plasma in pure hydrogen at atmospheric pressure. Contrib. Plasma Phys. **54**(2), 138–144 (2014)